Journal of Materials Chemistry B

Accepted Manuscript

ROYAL SOCIETY OF CHEMISTRY

www.rsc.org/materialsB

Cite this: DOI: 10.1039/c0xx00000x

www.rsc.org/xxxxxx

ARTICLE TYPE

Thermoresponsive PNIPAAm hydrogel scaffolds with encapsulated AuNPs show high analyte trapping ability and tailored plasmonic properties for high sensing efficiency.

A.C. Manikas[a], A. Aliberti[a], F. Causa[a,b,c], E. Battista[a] and P.A. Netti[a,b,c]

Received (in XXX, XXX) Xth XXXXXXXXX 20XX, Accepted Xth XXXXXXXXX 20XX
DOI: 10.1039/b000000x

The fabrication of a scaffold able to control the positioning of AuNPs and to trap and concentrate target molecules inside them is a promising idea for a large variety of sensing applications. In this work, we designed and fabricated a scaffold of already prepared 20 nm AuNPs encapsulated in a PNIPAAm hydrogel and utilizing Surface Enhanced Raman Spectroscopy (SERS) we used it as a sensor with remarkably low limits of detection. In fact, as the target is trapped inside the hydrogel a) the concentration of the target increases dramatically and b) the localization of the AuNPs and thus of the hot-spots (areas with extremely high SERS enhancement factors) work synergically, improving the sensing ability of the scaffold. The SERS enhancement ability of our scaffolds was checked with adenine, 2-naphanelethiol and melamine molecules; the trapping efficiency was investigated for the melamine and a partition coefficient of $k=5x10^5$ was found. Finally, by focusing on a single PNIPAAm hydrogel with encapsulated AuNPs, we managed to detect 10^{-6} M -or else 10^8 molecules- of melamine trapped inside the scaffold.

Introduction

During the past decade smart hydrogels have drawn enormous research interest in the biomedical and pharmaceutical field because they can adjust their volume and their properties in response to ambient stimuli.[1,2] Among them, poly(N-isopropylacrylamide) (PNIPAAm) has been studied in detail with regard to its well-known phase behaviour in aqueous solutions, which has the sharpest transition in the class of thermo-sensitive alkylacrylamide polymers.[3,4] Indeed, it undergoes a reversible phase transition -from a swollen to a shrunken state when increasing temperature- at about 32 °C in pure water. Below this temperature, called lower critical solution temperature (LCST), PNIPAAm is hydrated and its chains are in an extended conformational state. Above LCST, the hydrogel gets dehydrated and collapses due to the breaking down of the hydrophilic–hydrophobic balance in its network structure. Dehydration takes place in the PNIPAAm, resulting in the aggregation of the PNIPAAm chain and leading to the shrinking of the hydrogel. These phase transitions induce dramatic modifications in the optical properties of the substrate.[5]

Metallic nanoparticles (MNPs) possess distinct physical and chemical attributes that make them excellent scaffolds for the fabrication of novel chemical and biological sensors.[6-8] MNPs can be in fact synthesized in a straightforward manner and made highly stable. Also, they possess unique optoelectronic properties and provide high surface-to-volume ratio with excellent biocompatibility using appropriate ligands.[9] Such properties can be readily tuned by varying MNP size, shape, and the surrounding chemical environment. For example, the binding event between the recognition element and the analyte can alter physicochemical properties of transducer AuNPs, such as plasmon resonance absorption, conductivity, redox behaviour, etc., that in turn can generate a detectable response signal. MNPs can be multifunctionalized with a wide range of organic or biological ligands for the selective binding and detection of small molecules and biological targets.[10,11] In the past decade of research, the advent of MNP as a sensory element has allowed for a broad spectrum of innovative approaches for the detection of metal ions, small molecules, proteins, nucleic acids, malignant cells, etc., in a rapid and efficient manner.[12]

Many hybrid materials are based on the polymer coating of preformed nanoparticles[13-15] or the *in situ* synthesis of inorganic nanoparticles within a polymer matrix.[16-18] So far, only a few studies[19,20] have dealt with the loading of microgels with preformed nanoparticles. Lyon et al. loaded microgel particles with AuNPs in order to prepare hybrid materials for photo thermal patterning of colloidal crystals[20] and for light induced microlens formation.[21] It was demonstrated that strong illumination of a small region of a concentrated sample leads to photo thermal crystallization. However, neither the internal structure of the AuNP loaded microgels, nor any plasmon coupling effects during the volume phase transition of the AuNPs were investigated. Kumacheva et al. attached gold nanorods to copolymer microgels[22] and showed that laser excitation of the longitudinal plasmon resonance of the gold nanorods can be used to induce a collapse of the microgel core. The optical properties of the hybrid particles during the volume phase transition were,

however, not discussed. Using an approach similar to that of Kumacheva et al., Karg et al. attached polyelectrolyte-coated gold nanorods to the surface of oppositely charged microgels[23,24] and the optical properties of the gold nanorods were studied as a function of microgel swelling. The microgel collapse led to a significant decrease in the surface area, thus reducing the distance among the attached gold nanorods. Plasmon coupling was observed below a certain nanorods spacing and the longitudinal plasmon resonance was found to be significantly red shifted. Gawlitza et al. have recently presented the plasmon coupling induced by an increase in temperature where AuNPs concentration and/or cross linker density are directly related to the formation of dimmers of AuNPs.[25] To the best of our knowledge, no one until now has ever reported SERS experiments exploiting the plasmon coupling induced by temperature increase inside hybrid PNIPAAm-AuNPs templates. In our latest study we have already presented a new method for easy and fast physisorption of AuNPs on the surface of PNIPAAm hydrogels and the formation of high efficient SERS substrates.[26] We now approach the challenging task of combining the control over AuNP positioning and the capacity to trap[27] and concentrate target molecules inside the scaffold. A new scaffold of 20 nm AuNPs encapsulated in a PNIPAAm hydrogel can be used as a sensor with low expected limits of detection. In fact, the increment of the trapped target and the localization of the hot-spots (areas with extremely high SERS enhancement factors) inside the hydrogels work synergically and improve the sensing ability of the scaffold.

The so prepared scaffolds can be used for a large variety of applications because of the physical and chemical characteristics of both AuNP and PNIPAAm hydrogels. We used them as sensors for the detection of different molecules by Surface Enhanced Raman Spectroscopy because of their ability to localize the AuNPs within polymer matrixes and tuning their interparticle distance, thus inducing plasmon coupling.

Experimental

A. Materials

N-Isopropylacrylamide (97%) (NIPAM), N,N'-Methylenebis(acrylamide) (BIS) (≥ 99.5%), potassium peroxodisulfate (KPS) (≥ 99%), adenine, melamine and 2-naphthanelenthiol were purchased from Sigma-Aldrich (Munich, Germany). Gold nanoparticles (AuNPs) were from BBInternational. All the chemicals were used as received. A Millipore Milli-Q Plus 185 purification system was used for water purification.

Synthesis of PNIPAAm microgel particles: The PNIPAAm microgels were synthesized by free radical precipitation polymerization.[28-30] Polymerization was conducted in a 200 mL three-necked flask equipped with a condenser and a stirrer. Briefly, 0.975 g of NIPAM, 0.025 g of BIS were dissolved in 95 mL of water. The solution was filtered to remove any possible precipitates. The reaction mixture was transferred to a three-necked round-bottom flask equipped with a condenser and a nitrogen inlet and heated to 70 °C under a gentle stream of nitrogen. After 1 h, 5 mL of 0.06 M KPS solution were added to initiate the reaction. The reaction was allowed to proceed for 5 h. The resulting microgels were purified by dialysis (cut off 12 000-14 000 MW) against water for at least 1 week. This PNIPAAm microgel sample has a feeding BIS content of 2.5 wt %. Microgels with BIS contents of 4.5 wt % were synthesized using the same procedure, but different feeding amounts of BIS.

Loading of PNIPAAm microgel particles with Au-NPs: the incorporation of the Au-NPs into the microgels was achieved by adding 0.100mL of the Au-NPs to 0.010mL of PNIPAAm microgel solution. This mixture was sonicated for 10 min using an ultrasonic bath and then centrifuged at 8000 rpm for 4 min. The residue obtained was then re-dispersed in 0.100 mL water.

B. Methods

Particle mass determination: Ubbelohde viscometer was used for determining intrinsic viscosity of different microgel preparation as already described by Romeo *et al*.[31]

Using the Einstein-Batchelor relation:

$\eta_r = 1+2.5\ (kxc)+B\ (k\ xc)^2$

The data were fitted at fixed temperature to obtain the intrinsic volume fraction:

$k = \zeta/c$

Since the solution density is essentially equal to that of water, $\rho = 1 g\ cm^{-3}$, the intrinsic volume fraction becomes:

$k = \zeta/c = v/ m_p$

with v the particle volume and m_p its mass.

K values were calculated by viscosimetry and the volume of the particles v using dynamic light scattering measurements.

Dynamic Light Scattering: The swelling efficiency of pure and AuNPs-loaded hydrogels was investigated with Dynamic Light Scattering. DLS measurements were performed with an ALV – CGS-3 compact goniometer (ALV-Laser GmbH, Langen, Germany) operating at a wavelength of 633nm in vacuum and a time correlator ALV – LSE-5003 (ALV-Laser GmbH, Langen, Germany). The correlation functions were recorded at a constant scattering angle of 90°. The measurements were carried out over a temperature range from 20 to 50 °C using a thermo stated bath.

Transmission Electron Microscopy: The AuNPs loading was investigated by Transmission Electron microscopy. Electron microscopy specimens were prepared using 5 µL of solution on a TEM copper grid with carbon support (200 mesh, Agar scientific). After solution evaporation the grid was washed with deionized water in order to remove salt excess from the grid surface. Scanning transmission electron microscopy was performed with a Cryo-TEM tomography TECHNAI 20 FEI COMPANY. The images were acquired on a Vacuum generator operated at 250KV with camera (FEI-EAGLE) exposure time of 1 sec. The estimated point to point resolution was 2 A.

UV-Vis absorption spectroscopy: The coupling of the surface plasmon because of the hydrogel collapsing was examined by UV-Vis absorption Spectroscopy. UV-Vis absorption spectroscopic measurements were performed on PNIPAAm-AuNPs solutions that were placed in 1 cm path-length quartz optical cuvettes. Spectra were recorded with a Cary 100 UV-Vis spectrometer from 400 to 800 nm. The estimated resolution was 1 nm and as the background was corrected with Milli Q water. The measurements were carried out over a temperature range from 20 to 50 °C using a thermo stated bath.

Raman Spectroscopy: The Raman spectra were excited with diode lasers of 633 nm and 780 nm. A 10x/0.25 and a 50x/0.50 LWD objective were used to focus the laser beam into the well plate and inside the capillary. The Raman spectra were acquired with a DXR Raman spectrometer from Thermofischer Scientific with 20 mW laser power.

High-performance liquid chromatography: Partition of melamine between solution and microgel suspension was assessed by RP-HPLC (Waters equipped with 600 series Pumps and a Photodiode Array detector (Waters 2996)) using a X-Bridge BEH300 C18 3.5µm 4.6x250 column (Waters) in isocratic condition with acetonitrile 0,1% TFA over a period of 20 min (melamine R_t=7,6 min). The presented results an average of 3 measurements for each testing sample.

Result and discussion

Two PNIPAAm hydrogels with different cross-linker concentrations of 2.5 and 4.5% were synthesized by precipitation polymerization. The samples are denoted PNIPAAm(x), where x describes the cross-linker concentration. The hydrodynamic radii were measured by DLS in a temperature range of 20 to 50 °C from the fully swollen to the fully collapsed state and the results are presented in figure 1. The particle mass necessary for the determination of the particle concentration was calculated using the Ubbelohde viscometer. The mesh size was also calculated as reported by Saunders[32] and found to be ~2nm and ~1.5nm for PNIPAAm(2.5) and PNIPAAm(4.5), respectively. The results are presented in table 1.

A deep characterization of the AuNPs is helpful before incorporating them in the PNIPAAm hydrogels. Specifically, TEM, UV-Vis spectroscopy and DLS measurements were performed in the AuNP solutions. Figure 2 shows a representative TEM image of the particles and a UV-Vis absorption spectrum with the typical absorption band at around 520 nm. The diameter of the particles measured from DLS is around 19.3nm. The ζ-potential was also measured at 25 °C and found to be -36 mV.

Table 1 Mass, concentration and calculated mesh size of the synthesized PNIPAAm hydrogels

	PNIPAAm(2.5)	PNIPAAm(4.5)
Particle mass (gr)	$2.58X10^{-12}$	$8.45X10^{-12}$
Particle concentration ($N_{particles}$/mL)	$2.48X10^{9}$	$7.57X10^{8}$
Particle mesh size (nm)	2	1.5

Based on these results, we realized that it is impossible to physically trap the AuNPs inside the hydrogel because of the much higher dimensions of the nanoparticles compared to the hydrogel mesh size. So, an external stimulus was essential to force the AuNPs into the hydrogel and create the hybrid materials. Sonication was chosen as the external stimulus and the results are presented above.

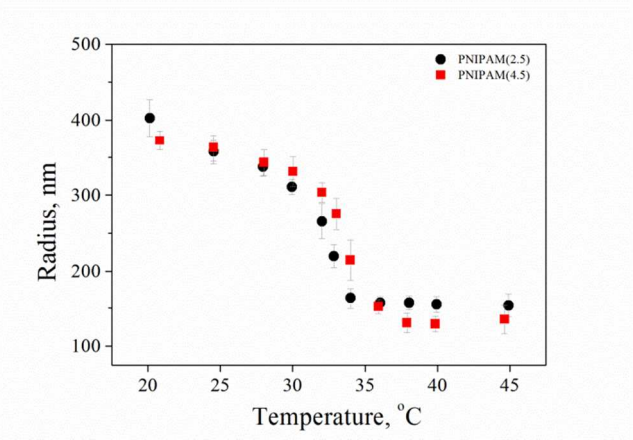

Fig1. Temperature dependence of the radius of PNIPAAm(2.5) and PNIPAAm(4.5) hydrogels

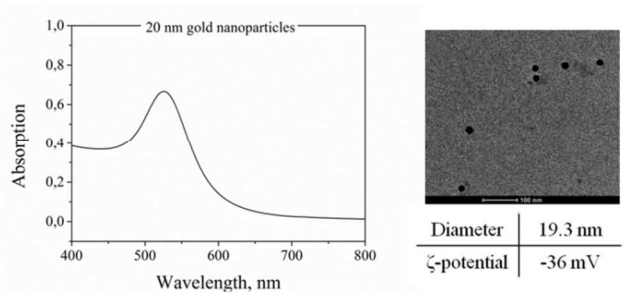

Fig. 2 UV-Vis absorption spectra and Transmission Electron images of 20nm AuNPs

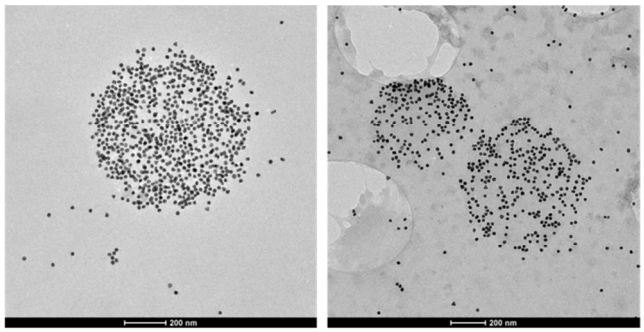

Fig.3 Transmission Electron images of loaded PNIPAAm(2.5) and PNIPAAm(4.5) hydrogels

Transmission Electron Microscopy images of loaded PNIPAAm(2.5) and PNIPAAm(4.5) hydrogels at 10 min of sonication time are presented in figure 3. We can see that the sonication allows the loading of the particles into the hydrogel. The PNIPAAm(2.5) hydrogel showed a better loading efficiency because of its bigger mesh size and higher flexibility and was used for the following experiments.

Thermoresponsive PNIPAAm-AuNPs composites were characterized by dynamic light scattering. Figure 4 exhibits the variation of the hydrodynamic radius of PNIPAAm-AuNPs templates as the temperature rises from 15 to 40 °C. The critical temperature for our system was at around 33 °C, where the radius changed rapidly. Since the measured LCST is similar to that of the pure PNIPAAm hydrogel, the presence of Au nanoparticles does not significantly affect the swelling behavior of the

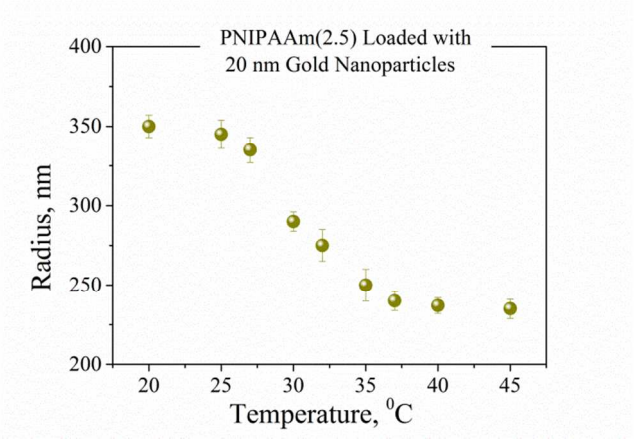

Fig.4 Temperature dependence of the radius of loaded PNIPAAm(2.5) hydrogels

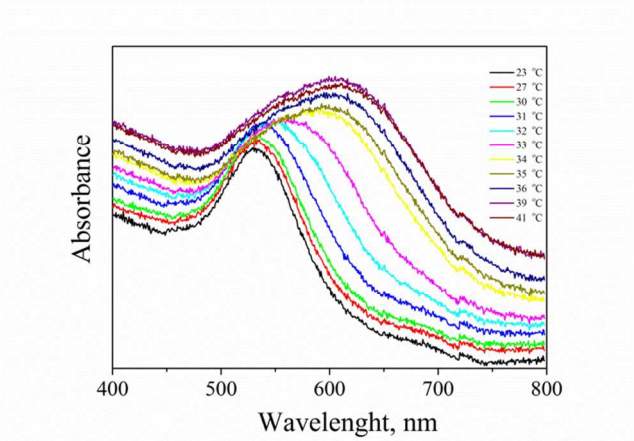

Fig.5 UV-Vis absorption spectra of loaded PNIPAAm(2.5) upon temperature changes

PNIPAAm template. Specifically, the radius measured 340 nm for the completely swollen hydrogels at 15 °C and 230 nm for the collapsed ones at 40 °C, as clearly demonstrated in figure 4. The polydispersity of the synthesized templates measured 16% at LCST higher than before the AuNPs adsorption that was 11%.

After verifying that the AuNPs were loaded inside the PNIPAAm hydrogel and after examining the size changes upon temperature variations, we investigated the plasmonic coupling of the surface plasmons. UV-Vis measurements were carried out on the aforementioned system at different temperatures and presented in figure 5. The differences on plasmon resonance of AuNPs in the PNIPAAm hydrogel were fundamental for the fabrication of SERS active substrates. It is clearly demonstrated in figure 5 that the absorption band of AuNPs at 525 nm change as temperature increases. More specific, a continuous broadening of the band is visible until LCST; above LCST changes are intense and the central absorption is red shifted at around 620 nm. Such red shift results from the coupling of surface plasmons between closely spaced particles; as the temperature rises, the distance between the AuNPs shortens. In aggregated colloids the particles are physically connected, but it is essential to note that direct contact is not always needed to observe collective plasmon modes. In fact, as long as the spacing between particles narrows compared to the wavelength of light, these collective plasmon modes can be

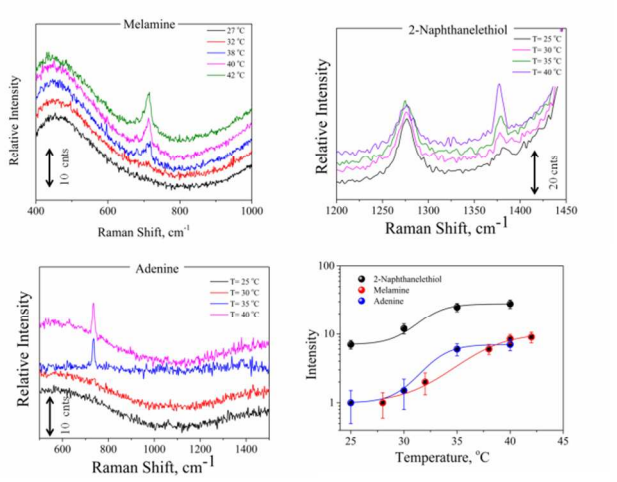

Fig6. Representative SERS spectra of Melamine, 2-Naphthanelenthiol, adenine and also the intensity dependence on temperature changes

observed. In this case, when the AuNPs-PNIPAAm template radius decreases, the interparticle spacing becomes narrow resulting in the red shift of the absorption band.

The SERS efficiency of the fabricated hydrogel scaffolds was tested by different target molecules, such as adenine, melamine and 2-naphthanethiol. 3×10^{-6} M of adenine solution, 10^{-5} M melamine solution and 10^{-6} M of 2-naphthanethiol were added to PNIPAAm-AuNPs composites and let diffuse inside them. 100 µL (50 µL of PNIPAAm-AuNPs and 50 µL of the target molecule) of this solution were placed under the microscope in a well plate. The spectra were collected using a 10X/x0.25 objective at different temperatures. Representative spectra are presented in figure 6 demonstrating the intensity dependence upon temperature changes. As it is clearly shown in figure 6, the intensity of the characteristic bands of each molecule at 20 °C is very low, but as temperature increases, the intensity also increases significantly. Such a result was expected because when the size of the composites decreases, the AuNPs come closer to each other creating hotspots and resulting in high enhancement on Raman spectra. Differences in each molecule's main peak intensity vs. temperature are also presented in figure 6.

As we mentioned above, this scaffold has the ability to trap and concentrate the target molecule. For the investigation of the concentrator efficiency we added 200 µL of 2 µg/mL of melamine solution in 200 µL of AuNPs-PNIPAAm hydrogels. 2 h after the melamine addition, the solution was centrifuged and the concentration of melamine on the supernatant solution was measured by HPLC. As it is presented in figure 7 such concentration was 0.45 µg/mL, meaning that a significant amount of the melamine got trapped inside the scaffold. Based on the amount of target inside a single hydrogel and its volume, a concentration of the target of 1 M was calculated on average in each single hydrogel. These values show that there is a relevant concentrator effect of the target inside the hydrogel; more specifically, a partition coefficient of $k=5x10^5$ was found as a ratio of the inner *to* outer melamine concentration. On average, of $4.8x10^{14}$ molecules added to the solution, $3x10^{14}$ were trapped in the scaffold, while $1.8x10^{14}$ remained in the solution. This concentration effect is due to the high affinity of AuNPs with the amines of the melamine molecules[33,34] that overcomes the

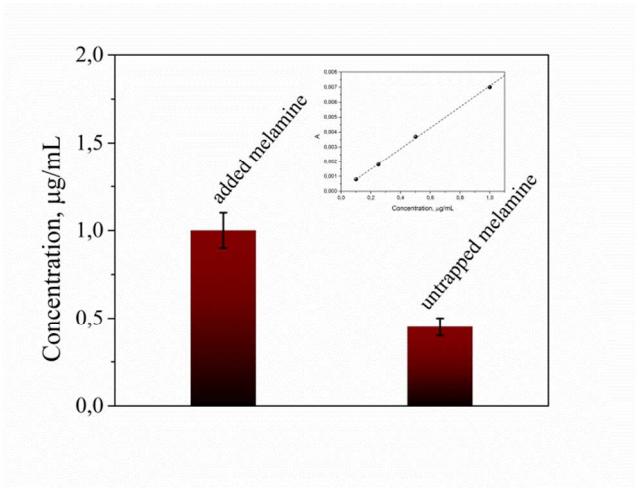

Fig.7 Determination of the untrapped melamine concentration with HPLC

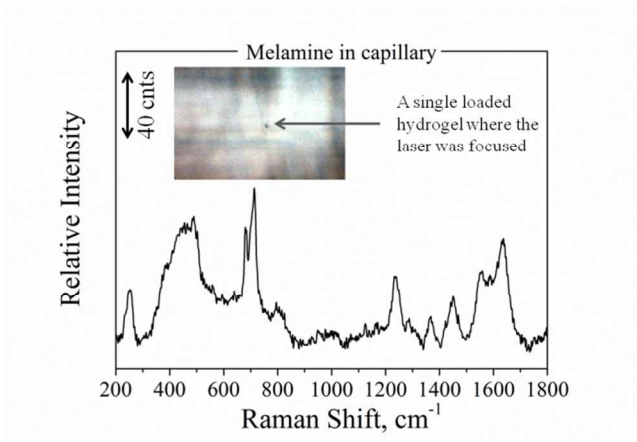

Fig.8 SERS spectra of melamine inside a glass capillary focused on a single loaded PNIPAAm hydrogel, as presented in the inset photo.

negative entropic contribution of the concentrating phenomenon. Taking in account the features of the fabricated scaffolds, we took one more step towards the improvement of their sensing efficiency. For the previous described SERS experiments we used 50 μL of PNIPAAm-AuNPs. Such volume contains around 10^6 PNIPAAm-AuNPs beads, but only a few of them interacted with focusing field of the laser and gave us the information of the SERS spectra. Therefore, we isolated and focused on a single AuNP loaded PNIPAAm hydrogel assuming to find similar spectra in a much lower amount of target molecule. To test our assumptions, we placed the melamine solution with the AuNPs loaded PNIPAAm hydrogels in vitrotubes® rectangular capillaries and under the microscope. After 1 h of adsorption of the hydrogels on the bottom surface of the capillary, we focused the laser line with a 50x/0.50 LWD objective on a single hydrogel. The recorded spectra and the image are presented in figure 8; as expected, the intensity of the spectra was much higher. Specifically, as it is clearly shown from the scale bars in figures 6 and 8, the increment of the melamine's Raman intensity, because of the better focusing, is around 4 times. In this case, the sensitivity of our system significantly increased and the LOD of the method now is less than 1μM much lower than the current melamine food safety requirements. Additionally, other melamine analytical methods[35,36] dealing with scaffold showed comparable or even higher LODs than what presented in this approach. Furthermore, in our case the easier sample handling could bring to direct and straightforward use in clinical or food testing applications. On the other hand, by focusing on a single hydrogel, the detectable quantity of melamine is extremely low and thus the experimental required amount of melamine was also much lower. Spectral contribution of melamine molecules outside the hydrogels was not possible because of the extremely low melamine concentration for the acquisition of conventional Raman spectra. The acquired spectra come exclusively from melamine molecules close to SERS active substrates, present only inside the loaded PNIPAAm-AuNPs hydrogels. The proposed experimental methodology offers the possibility for ultrasensitive detection thanks to the entrapment, the concentration of the target molecules inside the PNIPAAm-AuNP hydrogels and the activation of the hot-spots when increasing the temperature. This procedure can be generalized for a large number of molecules that can be trapped in our scaffold by physical adsorption, by diffusion, or even by chemical binding using gold nanoparticles conjugated with specific antibodies for more specific sensing applications. With the respect to the specificity, in the case of analogues of the target molecules or interferents Raman spectroscopy possesses the capability to discriminate even very similar molecules that might be trapped in the hydrogel template.

Conclusions

In conclusion, in this work we designed and fabricated new scaffolds of 20 nm AuNPs encapsulated in a PNIPAAm hydrogel that can be used for a large variety of sensing applications. In our case, such scaffolds were used as sensors for the detection of different molecules by Surface Enhanced Raman Spectroscopy because of the ability to localize the AuNPs within polymer matrixes and tune their interparticle distance, thus inducing plasmon coupling. In fact, as the target is trapped inside the hydrogel a) its topical concentration increases dramatically and b) the presence of the AuNPs and their localization inside the thermoresponsive scaffold generates hot-spots (areas with extremely high enhancement factors) upon temperature variations. These two factors work synergically improving significantly the sensing ability of the scaffold. Furthermore, by focusing on a single loaded hydrogel, we further improved the sensitivity of the system around 4 times because of the better focusing and reduced sampling volume. This approach can be adopted for every molecule with specificity on AuNPs or on PNIPAAm hydrogels in which it can be trapped, with extremely low limits of detection. Chemical modifications of the hydrogels or of gold nanoparticles could also increase significantly the number of different target molecules that can be trapped inside them making detection possible at extremely low concentration levels.

Notes and references

[a]*Center for Advanced Biomaterials for Healthcare@CRIB, Istituto Italiano di Tecnologia (IIT), Largo Barsanti e Matteucci 53, 80125 Naples, Italy*
[b]*Interdisciplinary Research Centre on Biomaterials (CRIB), University ''Federico II'', Piazzale Tecchio 80, 80125 Naples, Italy Optional Dedication))*
[c] *Dipartimento di Ingegneria chimica, dei Materiali e della Produzione industriale, Piazzale Tecchio 80, 80125 Naples, Italy*

1 D. Q. Wu, Y. X. Sun, X. D. Xu, S. X. Cheng, X. Z. Zhang, R. X. Zhuo, *Biomacromolecules*, **2008**, *9*, 1155
2 J. Zhang, N. A. Peppas, *Macromolecules,* **2000**, *33*, 102
3 T. Wu, Q. Q. Zhang, J. M. Hu, G. Y. Zhang, S. Y. Liu, *J. Mater. Chem.,* **2012**, *22*, 5155
4 J. H. Kim, T. R. Lee, *Langmuir*, **2007**, *23*, 6504
5 R. A. Alvarez-Puebla, R. Contreras-Caceres, I. Pastoriza-Santos, J. Perez-Suste, L. M. Liz-Marzan, *Angew. Chem., Int. Ed.,* **2009**, *48*, 138
6 E. Boisselier, D. Asturc, *Chem. Soc. Rev.*, **2009**, *38*, 1759.
7 H. Haick, *J. Phys. D: Appl. Phys,* **2007**, *40*, 7173
8 M. Zayats, R. Baron, I. Popov, I. Willner, *Nano Lett.*, **2005**, 5, 21
9 M. C. Daniel, D. Astruc, *Chem. Rev.*, **2004**, *104*, 293.
10 S. H. Radwan, H. M. E., *Expert Rev. Mol. Diagn.*, **2009**, *9*, 511
11 A. C. Manikas, F. Causa, R. Della Moglie, P. A. Netti, *ACS Applied Materials & Interfaces,* **2013**, *5*, 7915-7922
12 R. Wilson, *Chem. Soc. Rev.*, **2008**, *37*, 2028.
13 R. Contreras-Caceres, A. Sanchez-Inglesias, M. Karg, J. Perez-Juste, J. Pacifico, T. Hellweg, A. Fernandez-Barbero, L. M. Liz-Marzan, *Adv. Mater.,* **2009**, *20*, 1666
14 M. Karg, I. Pastoriza-Santos, L. M. Liz-Marzan, T. Hellweg, *ChemPhysChem*, **2006**, *7*, 2298
15 M. Karg, S. Jaber, T. Hellweg, P. Mulvaney, *Langmuir*, **2011**, *27*, 820
16 A. Pich, A. Karak, Y. Lu, A. K. Ghosh, H. J. P. Adler, *Macromol. Rapid Commun.,* **2006**, *27*, 344
17 Y. Lu, S. Proch, M. Schrinner, M. Drechsler, R. Kempe, M. Ballauff, *J. Mater. Chem.,* **2009**, *19*, 3955
18 H. Lange, B. H. Juarez, A. Carl, M. Richter, N. G. Bastus, H. Weller, C. Thomsen, R. Von Klitzing, A. Knorr, *Langmuir,* **2012**, *24*, 8862
19 J.H. Lee, A. M. A. Mahmoud, V. Sitterle, J. Sitterle, J. Carson Meredith, *J. Am. Chem. Soc.*, **2009**, *131*, 5048
20 C. Jones, L. Lyon, *J. Am. Chem. Soc.,* **2003**, *125*, 460
21 C. Jones, M. Serpe, L. Schroeder, L. Lyon, *J. Am. Chem. Soc.,* **2003**, *125*, 5292
22 M. Das, N. Sanson, D. Fava, E. Kumacheva, *Langmuir,* **2007**, *23*, 196
23 M. Karg, I. Pastoriza-Santos, J. Perez-Juste, T. Hellweg, L. M. Liz-Marzan, *Small*, **2007**, *3*, 1222
24 M. Karg, Y. Lu, E. Carb-Argibay, I. Pastoriza-Santos, J. Perez-Juste, L. M. Liz-Marzan, T. Hellweg, *Langmuir,* **2009**, *25*, 3163
25 K. Gawlitza, S. T. Turner, F. Polzer, S. Wellert, M. Karg, P. Mulvaney, R. Von Klitzing, *Phys.Chem. Chem. Phys.,* **2013**, *15*, 15623
26 A. C. Manikas, G. Romeo, A. Papa, P. A. Netti, *Langmuir,* **2014**, *30*, 3869
27 R. Riahi, K. E. Mach, R. Mohan, J. C. Liao, P. K. Wong, *Anal Chem.,* **2011**, *83*, 6349
28 M. J. Sepre, C. D. Jones, L. A. Lyon, *Langmuir*, **2003**, *19*, 8759
29 X. J. Gong, C. Wu, T. Ngai, *Colloid Polym. Sci.,* **2010**, *288*, 1167
30 C. Jones, L. Lyon, *Macromolecules,* **2000**, 33, 8301
31 G. Romeo, L. Imperiali, J. Kim, A. Fernandez-Nieves, D. A. Weitz, . *Chem. Phys.,* **2012**, *136*, 124905
32 B. R. Saunders, *Langmuir,* **2004**, *20*, 3925
33 A. Kumar, S. Mandal, P. R. Selvakannan, R. Pasricha, A. B. Mandale, M. Sastry, *Langmuir*, **2003**, *19*, 6277
34 D. V. Leff, L. Brandt, and J. R. Heath, *Langmuir*, **1996**, *12*, 4723
35 J. M. Li, W. F. Ma, C. Wei, L. Y. You, J. Guo, J. Hu, C. C. Wang, *Langmuir*, **2011**, *27*, 14539
36 J. F. Betz, Y. Cheng, G. W. Rubloff, *Analyst*, **2012**, *137*, 826

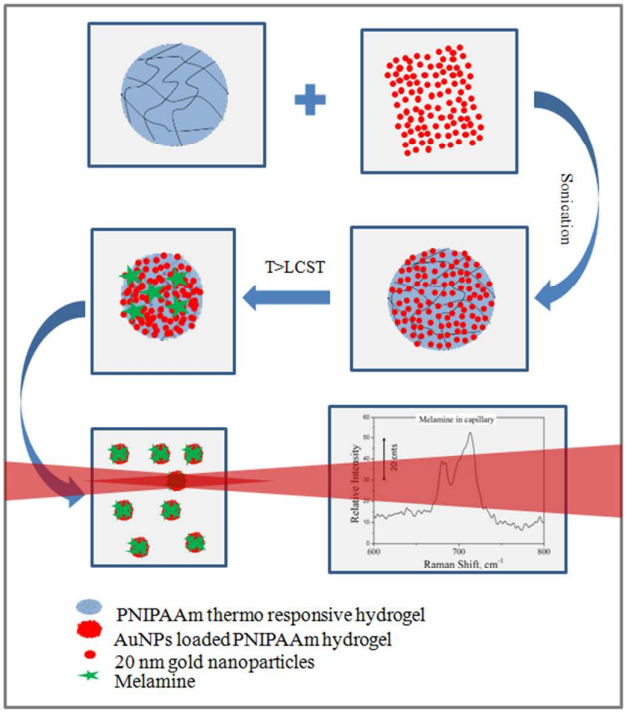

The preparation of thermoresponsive PNIPAAm hydrogel scaffolds with encapsulated AuNPs showed high analyte trapping ability and tailored plasmonic properties with high sensing efficiency